



# Two three-dimensional silver(I) coordination architectures with pyridine-3,5-dicarboxylate: Luminescence and structural dependence on preparing conditions

Ya-Bo Xie<sup>\*</sup>, Qian Gao, Chao-Yan Zhang, Ji-Hong Sun<sup>\*</sup>

College of Environmental and Energy Engineering, Beijing University of Technology, Beijing 100124, PR China

## ARTICLE INFO

### Article history:

Received 28 November 2008

Received in revised form

11 March 2009

Accepted 5 April 2009

Available online 18 April 2009

### Keywords:

Pyridine-3, 5-dicarboxylate

Hydrothermal reactions

Crystal structures

Three-dimensional frameworks

Luminescent properties

## ABSTRACT

The hydrothermal reactions of pyridine-3,5-dicarboxylic acid ( $H_2pydc$ ) with  $AgNO_3$  in the mixed solvent of acetonitrile and water with different ratios lead to the formation of two three-dimensional network complexes,  $[Ag_5(pydc)_2(CN)]_n$  (**1**) and  $\{[Ag_4(pydc)_2]CH_3CN\}_n$  (**2**), which have been characterized by IR, single-crystal X-ray diffraction and thermogravimetric analyses. It has been demonstrated that the ratio of acetonitrile and water have great effect on the structures of products. The high ratio of acetonitrile and water is favorable for the formation of complex **1**, while the low volume ratio is propitious to complex **2**. The luminescent properties of complex **1** and **2** have been further investigated, and show that the luminescence intensity of **2** is much stronger than that of **1** probably due to the direct metal–metal interactions and a larger HOMO–LUMO gap in complex **2**.

© 2009 Elsevier Inc. All rights reserved.

## 1. Introduction

Research has commenced a number of approaches towards the design and synthesis of metal-organic frameworks (MOFs) based on the concept of crystal engineering [1–3] due to the MOFs' greatly potential applications in various areas such as catalysis, magnetism, gas storage, and luminescence, etc. [4–10]. The challenge for this work is to exactly control the structures of the target products and build the relationship between structures and physicochemical properties. To our knowledge, the self-assembly of metal ions and ligands forming topology of coordination polymer is highly influenced by various factors such as the selection of proper metal ions, solvent system, template, the molar ratio of the reagents, and pH value of the solution [11–13].  $Ag(I)$  ion with a  $d^{10}$  electronic configuration exhibits irregular coordination geometries and can greatly accommodate to many kinds of ligands. The reported structures of  $Ag(I)$  ion complexes cover from the discrete to 3D structures [12,14,15]. Particularly, the interleaving of helical chains, short  $Ag \cdots Ag$  separations and regular channels in three-dimensional (3D) structure play a crucial role in manifestation of luminescence properties [14,16].

As a multidentate ligand, pyridine-3,5-dicarboxylic acid ( $H_2pydc$ ), has displayed its diversiform coordination modes with

calcium(II) [17] and tetrabromoaurate(III) ions [18]. However, the coordination features of this ligand, as well as the relationship between complex structures and various preparing conditions have not been widely investigated to date. In previous works, the similar ligand, pyrazine-2-carboxylic acid has coordinated to  $Ag(I)$  ions forming interesting topology [19] and showing well luminescence [20]. Our idea in this work is to explore the synthesis of new MOF materials by  $H_2pydc$  and  $Ag(I)$  ions, and investigate the luminescent properties of these complexes. Herein, we report the syntheses, crystal structures and luminescent properties of two 3D  $Ag(I)$  complexes with  $pydc$  ligand obtained in different synthesis conditions.

## 2. Experimental

### 2.1. Materials and general methods

All reagents for syntheses and analyses were of analytical grade. Pyridine-3,5-dicarboxylic acid was purchased from Alfa Aesar Chem. Comp. FT-IR spectra (KBr pellet) were obtained on a FT-IR 170 SX (Nicolet) spectrometer. C, H, and N elemental analyses were performed on a Perkin-Elmer 240C analyzer. Thermogravimetric (TG) and differential thermal analyzer (DTA) were carried out in the temperature range 20–600 °C, with scan rate 10 °C/min, in an atmosphere of air. Powder X-ray diffraction (PXRD) patterns were recorded on BRUKER D8 ADVANCE X-ray

<sup>\*</sup> Corresponding authors. Fax: +86 10 67392130.

E-mail addresses: [xieyabo@bjut.edu.cn](mailto:xieyabo@bjut.edu.cn) (Y.-B. Xie), [jhsun@bjut.edu.cn](mailto:jhsun@bjut.edu.cn) (J.-H. Sun).

diffractometer with steccan scan type and 0.5 s/step scan speed at room temperature. The luminescence studies were carried out on powdered samples in the solid state at room temperature using a VARIAN Cary Eclipse spectrometer.

## 2.2. Synthesis of $[Ag_5(pydc)_2(CN)]_n$ **1** and $\{[Ag_4(pydc)_2]CH_3CN\}_n$ **2**

$[Ag_5(pydc)_2(CN)]_n$  (**1**), a mixture of  $H_2pydc$  (0.50 mmol) and  $AgNO_3$  (2.0 mmol) was placed in a sealed Teflon-lined stainless steel vessel (25 mL) containing 10 mL mixed solvent of acetonitrile and deionized water with the volume ratio of 4.5:1. The vessel was heated at  $140^\circ C$  for three days under autogenous pressure, and then cooled to room temperature. Yellow needle crystals of **1** were harvested in a yield of 64% based on  $Ag(I)$ . FT-IR (KBr disk,  $cm^{-1}$ , s: strong; m: middle; w: weak.): 3398(s), 2142(m), 1688(m), 1613(s), 1589(m), 1441(w), 1410(m), 1379(s), 1290(m), 1102(w), 1033(w), 828(w), 768(m), 725(m), 429(w). Anal. Found: C, 20.19; H, 0.71; N, 4.70. Anal. Calcd (%) for  $C_{15}H_6Ag_5N_3O_8$ : C, 20.12; H, 0.68; N, 4.69.

$\{[Ag_4(pydc)_2]CH_3CN\}_n$  (**2**), Complex **2** was prepared in the same manner as described for **1** except that the volume ratio of acetonitrile and deionized water is 1:1. Colorless block crystals of **2** were obtained in a yield of 58% based on  $Ag(I)$ . FT-IR (KBr disk,  $cm^{-1}$ , s: strong; m: middle; w: weak.): 3392(s), 1688(m), 1611(s), 1564(m), 1440(m), 1410(m), 1375(s), 1286(m), 1144(w), 1119(w), 1033(w), 922(m), 819(w), 768(m), 729(m), 434(w). Anal. Found: C, 19.50; H, 1.06; N, 4.54. Anal. Calcd (%) for  $C_{16}H_9Ag_4N_3O_8$ : C, 19.53; H, 0.98; N, 4.55.

## 2.3. Crystal structure determination

The single crystal X-ray diffraction measurement was carried out on a Bruker Smart 1000 diffractometer equipped with graphite-monochromatized  $MoK\alpha$  radiation ( $\lambda = 0.71073 \text{ \AA}$ ) with  $\omega$  scan mode at 293(2)K. The total of 15003 including 1923 independent reflections ( $R_{int} = 0.0702$ ) and 8384 including 1771 independent reflections ( $R_{int} = 0.0513$ ) were collected in the range of  $3.41 < \theta < 27.48^\circ$  for complex **1** and  $3.47 < \theta < 25.99^\circ$  for **2**, respectively. Largest diff. peaks and holes are 1.727 and  $-1.360 \text{ e \AA}^{-3}$  for **1** and 1.066 and  $-1.544 \text{ e \AA}^{-3}$  for **2**. Unit cell dimensions were obtained with least-squares refinements and multiscan corrections were applied using SADABS program [21]. The structure was solved by direct method [22] and non-hydrogen atoms were obtained in successive difference Fourier syntheses.

**Table 1**  
Crystallographic and experimental data for complexes **1** and **2**.

Compound	<b>1</b>	<b>2</b>
Formula	$C_{15}H_6Ag_5N_3O_8$	$C_{16}H_9Ag_4N_3O_8$
<i>M</i>	895.58	802.74
Crystal system	Orthorhombic	Monoclinic
Space group	<i>Pccn</i>	<i>C2/c</i>
<i>a</i> (Å)	6.7349(13)	12.889(3)
<i>b</i> (Å)	11.941(2)	15.266(3)
<i>c</i> (Å)	20.755(4)	10.389(2)
$\alpha$ (deg)	90	90
$\beta$ (deg)	90	118.06(3)
$\gamma$ (deg)	90	90
<i>V</i> (Å <sup>3</sup> )	1669.1(5)	1803.8(6)
<i>Z</i>	4	4
<i>D<sub>c</sub></i> (g cm <sup>-3</sup> )	3.564	2.956
$\mu$ (mm <sup>-1</sup> )	5.822	4.335
$\lambda$ (Å)	0.71073	0.71073
<i>T</i> (K)	293(2)	293(2)
Reflections collected	15003	8384
Observed data	1923	1771
<i>R</i> <sub>1</sub> ( <i>I</i> > 2 $\sigma$ )	0.0512	0.0502
<i>wR</i> <sub>2</sub> ( <i>I</i> > 2 $\sigma$ )	0.1822	0.1592

Hydrogen atoms of C were included in calculated positions and refined with fixed thermal parameters riding on their parent atoms. The final refinement was performed by full matrix least-squares methods with anisotropic thermal parameters for non-hydrogen atoms on  $F^2$ . Crystal parameters and structure refinement are summarized in Table 1. Selected bond distances and angles are listed in Tables S1 and S2.

## 3. Results and discussion

### 3.1. Synthesis consideration and general characterizations

Hydrothermal reaction has been proven to be a particularly useful technique in the synthesis of polymeric complexes. The specific hydrothermal environment benefits the process of merging molecular building blocks into an entity, especially, inorganic ions and organic ligands into a coordination framework. There are many factors affecting the formation and crystal growth of products, such as the pH value of solution, solvent system, temperature, reaction time, etc. [13,23,24]. In this case, the volume ratio of the solvents plays an important role in the formation of products. Complexes **1** and **2** were both obtained from the hydrothermal reactions of  $AgNO_3$  and  $H_2pydc$  ligand in  $H_2O$  and  $CH_3CN$  mixed solvent at  $140^\circ C$  for three days with differences only in the volume ratio of the two solvents. **1** is formed in the solvent system in which acetonitrile occupies a great proportion (A) while for **2** water occupies a great proportion (B). The different solvent system may offer different chemical/physical environments such as pressure in vessel, therefore producing different products. The solvent system of A has more acetonitrile, so it has lower boiled temperature than the solvent system of B. The solvent system of A may generate larger pressure than the solvent system of B in the sealed reactor at the same temperature ( $140^\circ C$ ). This may provide enough energy to break the C–C bond of  $CH_3CN$  molecule resulting in producing CN groups coordination to  $Ag(I)$  ions. The larger pressure may also provide proper energy to convert the coordination mode of  $pydc$  from low coordination number such as 2 or 4 to high coordination number 5 or even 6. The experimental results show that complex **1** was created at the volume ratio of the  $CH_3CN$  and  $H_2O$  more than 4:1, while complex **2** will be obtained at the volume ratio of  $CH_3CN$  and  $H_2O$  less than 2.5:1. Further experiment demonstrated that both complexes (as a mixture formed) can be obtained when the volume ratio of the  $CH_3CN$  and  $H_2O$  is used in the range from 4:1 to 2.5:1. TG analysis of **1** indicates that it begins to perform the chemical process of decomposition at about  $300^\circ C$ . While **2** is only stable up to  $150^\circ C$ , which can be seen from Fig. S1. PXRD patterns illustrate the powder samples of the two complexes match well with their simulated patterns from crystal data (Fig. S2).

### 3.2. Description of crystal structures

The structure of **1** is a 3D polymeric network in which there exist three crystallographic independent  $Ag(I)$  centers. As shown in Fig. 1a,  $Ag1$  (dark pink ball) and  $Ag2$  (light green ball) are five-coordinated in a slightly distorted trigonal-bipyramidal coordination environment.  $Ag1$  coordinates with four carboxylate O atoms from three ligands and one N atom from  $CN^-$  anion with O2, O3, and N2 occupying the equatorial positions and O1 and O2A residing in the axial positions.  $Ag2$  also coordinates three carboxylate O atoms from three ligands, one N atom from  $CN^-$ , and one N atom from ligand, but the atom connectivity is not the same as that of  $Ag1$ , with N1A, N2A, and O4B occupying the equatorial positions and O1B and O4 sitting on the axial positions. There exist  $\pi$ – $\pi$  stacking interactions between the aromatic rings of adjacent  $pydc$  ligands with a face-to-face

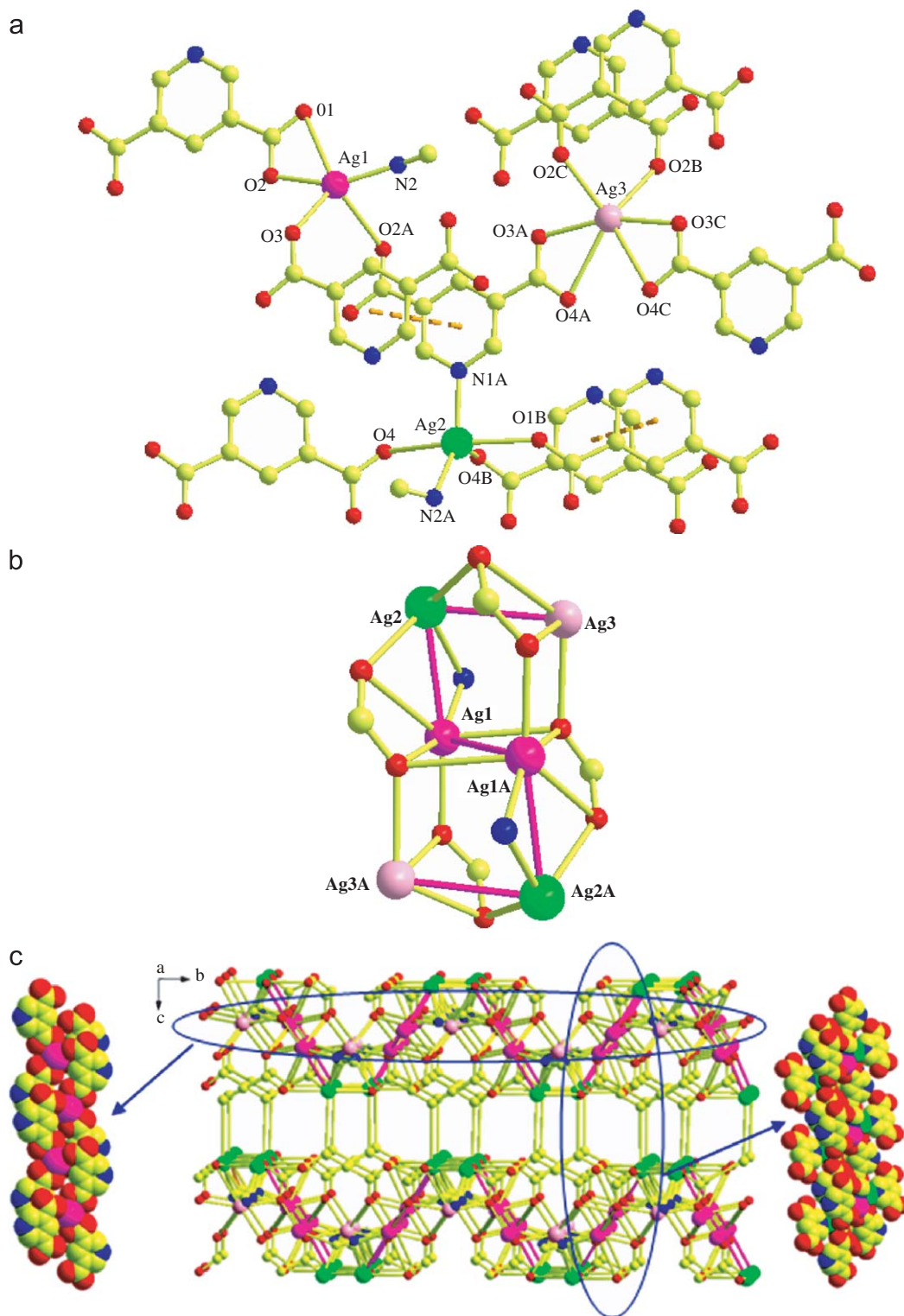
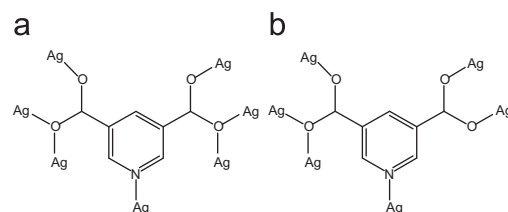


**Fig. 1.** (a) The view of the coordination geometry of Ag(I) in **1**. (b) The structure of  $[\text{Ag}_6(\text{COO})_4\text{N}_2]$  cluster. (c) The 3D structure of **1**.

distance of 3.641 Å [25,26]. Ag3 (light pink ball) is six-coordinated in a distorted octahedron coordination environment to six O atoms from four ligands. The distance of O4–Ag3 (2.804 Å) is longer than that of O2–Ag3 (2.517 Å) and O3–Ag3 (2.440 Å) indicating the weaker interaction. The distances of Ag1···Ag1A (3.0504 Å), Ag1···Ag2 (3.0566 Å), and Ag2···Ag3 (3.2316 Å) [27–30] are shorter than the van der Waals radii of two silver atoms (3.44 Å) [31,32] indicating the existence of Ag···Ag interactions which result in  $[\text{Ag}_6(\text{COO})_4\text{N}_2]$  cluster (Fig. 1b). In **1**,



**Scheme 1.** Coordination modes of pydca ligand in Crystal **1** and **2**.



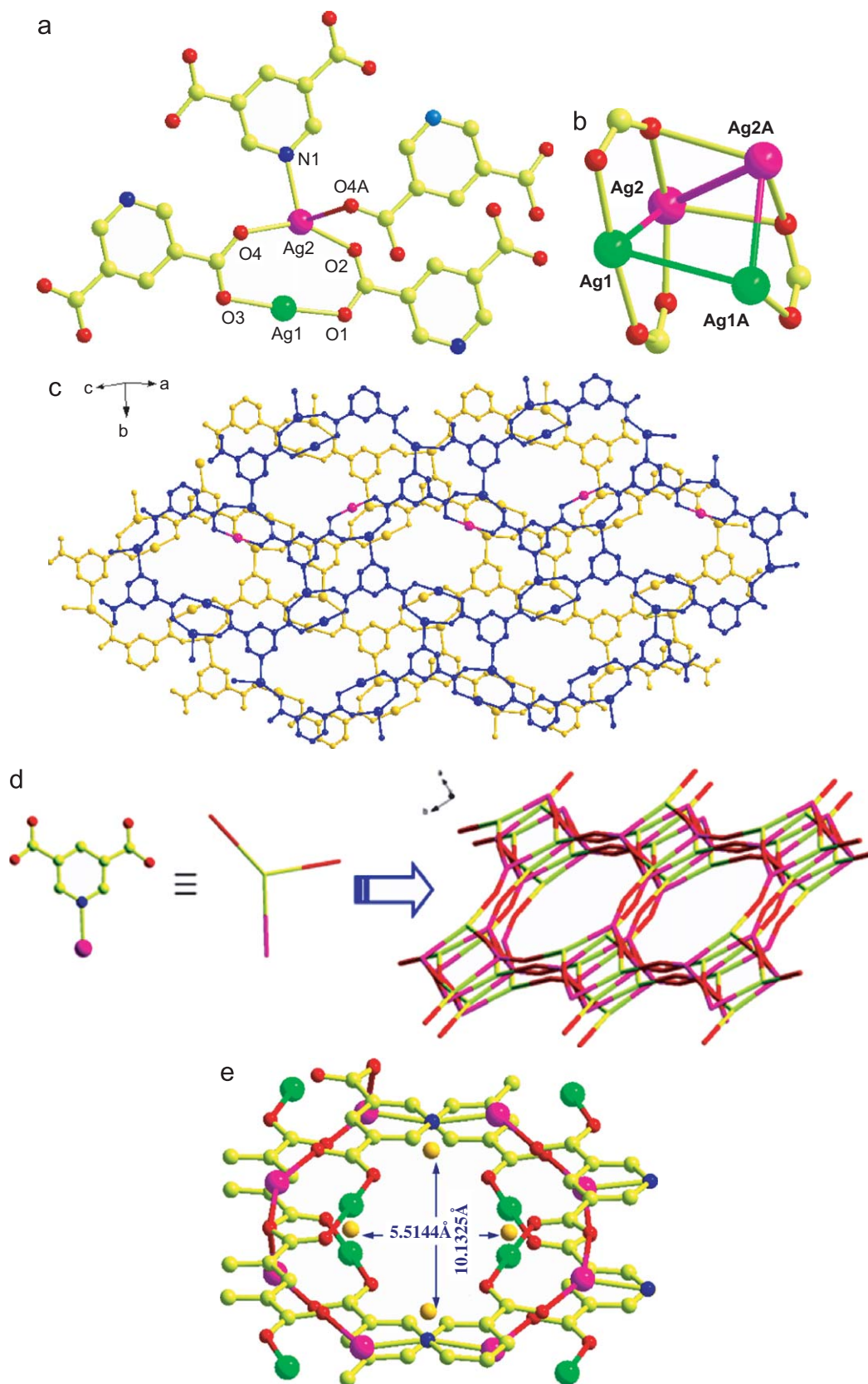


**Fig. 2.** (a) Perspective view of the coordination environment of Ag(I) in **2**. (b) The structure of  $[\text{Ag}_4(\text{COO})_3]$  cluster. (c) The 2D slabs in **2** (the disordered  $\text{CH}_3\text{CN}$  has been deleted for clarity). (d) The 3D network of **2**. (e) The dimension of the channel in **2** measured by atom-to-atom distances.

the ligand adopts only one kind of coordination mode, and each ligand provides five donor sites and connects with seven Ag(I) atoms as shown in Scheme 1a.

In Fig. 1c, two kinds of chains can be found in the 3D structure. One chain is formed by the zig-zag Ag1 and Ag2 clusters with the distance of  $\text{Ag2} \cdots \text{Ag2A}$  of 7.228 Å, and the repeating period in the

chains is about 18.720 Å (Fig. S3). The adjacent chains are antiparallel. The other is the Ag3 chain with the distance of Ag...Ag being 7.005 Å, and the repeating period in the chain is about 17.126 Å (Fig. S4). The weak interactions between Ag2 and Ag3 and the bonds of Ag2–N1 directly lead to the connection between the adjacent Ag3 chains, while Ag2 atoms also repeatedly appear as the start of the zig–zag Ag1, Ag2 cluster chain (Fig. S5). The two chains are attached to each other with coordination actions forming 3D network. In order to make it easily to image the structure of **1**, the “node and rod” topology can be seen in Fig. S6.

Complex **2** is also a 3D polymeric network. In **2**, there exist two crystallographic independent Ag(I) centers. As shown in Fig. 2a, Ag1 (light green ball) is in linear coordination environment and is coordinated to two carboxylate O atoms from two ligands. The distances of Ag1–O1 and Ag1–O3 are 2.137(5) and 2.159(4) Å, respectively. Ag2 (dark pink ball) has a distorted tetrahedral geometry being bound by three carboxylate O atoms from three discrete ligands and one N atom of the ligand with N1, O2, and O4 occupying the equatorial positions and O4A residing in the axial position. The angles around the Ag1 center are 64.79(15)° and 175.08(19)°, respectively, while that around the Ag2 center range from 56.03(13)° to 171.595(15)°. Ag1...Ag1A, Ag1...Ag2, and Ag1A...Ag2A distances [3.2381(16), 2.9166(9) and 2.9166(9) Å] are significantly shorter than the sum of the van der Waals radii for two silver atoms (3.44 Å) [31,32], indicating the weak interactions between adjacent Ag(I) atoms, which lead to form the [Ag<sub>4</sub>(COO)<sub>3</sub>] cluster (Fig. 2b). In **2**, ligand adopts one kind of coordination mode and provides five donor sites and connects with six Ag(I) centers as shown in Scheme 1b.

In the *ab* plane, complex **2** forms a 2D coordination slab substructure which is constructed from the junction of 8-membered [Ag1OCOAg2OCO] rings, 12-membered [(Ag2OC<sub>3</sub>N)<sub>2</sub>] rings, and 28-membered [(Ag2NC<sub>3</sub>OAg1OC<sub>5</sub>O)<sub>2</sub>] ellipsoids. The adjacent slabs exhibit the antiparallel manner (Fig. 2c). These fragments are further connected by the coordination of ligand with the axial bond Ag2–O4A (2.321(5) Å) [33]. (Fig. 2d) There exist the regularly elliptic channels in the network. In order to eliminate the intra-slab error in measuring the dimension of each channel, some imaginary atoms are inserted between the adjacent slabs. So the dimension is 10.1325 × 5.5144 Å measured by atom-to-atom distances (Fig. 2e), and the percent effective free solvent volume of 11.6% calculated with PLATON [34].

### 9>3.3. Luminescent properties

To our knowledge, Ag(I) complexes usually emit weak photoluminescence [35,36], and the room temperature luminescent properties of silver(I) complexes have been reported [37,38]. As shown in Fig. 3, **1** and **2** exhibit the blue/green photoluminescence at room temperature with the emission maximum at ca. 527 and 488 nm upon excitation at 387 and 332 nm, respectively. Noting that the free pydca ligand displays very weak luminescence in the solid state at ambient temperature with the emission maximum at ca. 378 nm, the enhancement of luminescence in **1** and **2** should be attributed to cluster-centred emission which have been reported as an important factor contributing to the photoluminescent properties of coinage *d*<sup>10</sup> metal coordination compounds [39,40] and accompanied by ligand-to-metal charge transfer (LMCT) transition mixed with *d*–*s* character [41–43]. It is noteworthy that the luminescence intensity of **2** (Fig. 3b) is much stronger than that of **1** (Fig. 3a). This suggests that the different three-dimensional architectures may course the different intensities of supramolecular interactions (such as  $\pi$ – $\pi$  interaction, Ag...Ag interaction), which can result in the different HOMO–LUMO gap [44–46]. On the other hand, the connection between CN<sup>–</sup> and Ag(I) in **1** also could disrupt the intermolecular

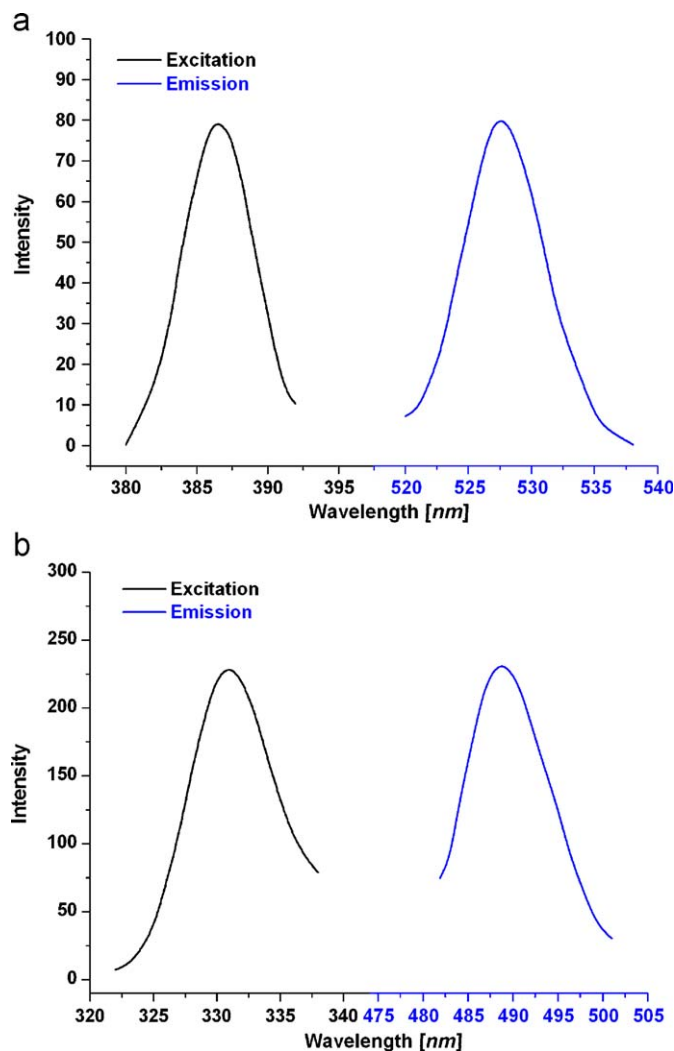


Fig. 3. The solid-state excitation (left) and emission (right) spectra of **1** (a) and **2** (b).

Ag–Ag interaction, which could consequently affect the  $4d^* \rightarrow 5p\delta$  transition [37].

## 4. Conclusions

In this paper, we have successfully synthesized and characterized two 3D complexes, [Ag<sub>5</sub>(L)<sub>2</sub>(CN)<sub>n</sub> (**1**) and {[Ag<sub>4</sub>(L)<sub>2</sub>CH<sub>3</sub>CN]<sub>n</sub> (**2**). In **1**, two kinds of chains named [Ag<sub>4</sub>(COO)<sub>2</sub>(CN)<sub>2</sub>] cluster chain and Ag3 chain are attached to form 3D structure. In **2**, ligands link Ag(I) centers to form a 2D slab in the equatorial plane of the tetrahedral coordination Ag2 atoms, while the axial Ag2–O4 bonds finally build up the 2D networks into a 3D structure. Both **1** and **2** exhibit the blue/green photoluminescence at room temperature with the emission maximum at ca. 527 and 488 nm upon excitation at 387 and 332 nm, respectively. The luminescence intensity of **2** is much stronger than that of **1** probably due to the direct metal–metal interactions and a larger HOMO–LUMO gap in **2**.

## Supplementary data

CCDC-684327, and 684328 contains the supplementary crystallographic data for complex **1** and **2**. These data can be obtained from the Cambridge Crystallographic Data Centre, 12 Union Road,

Cambridge CB2 1EZ, UK; Fax: +44-1223-336033; E-mail: deposit@ccdc.cam.ac.uk.

## Acknowledgments

This work was supported Beijing Municipal Natural Science Foundation (No. 2082004) and the Major State Basic Research Development Program of China (973 Program, No. 2009CB930200).

## Appendix A. Supplementary data

Supplementary data associated with this article can be found, in the online version, at [10.1016/j.jssc.2009.04.012](http://10.1016/j.jssc.2009.04.012).

## References

- [1] S.L. Childs, L.J. Chyall, J.T. Dunlap, V.N. Smolenskaya, B.C. Stahly, G.P. Stahly, *J. Am. Chem. Soc.* 126 (2004) 13335–13342.
- [2] B. Kumar, S. Madhushree, R. Lalit, *Chem. Commun.* 40 (2006) 4169–4179.
- [3] S.A. Dalrymple, G.K.H. Shimizu, *J. Am. Chem. Soc.* 129 (2007) 12114–12116.
- [4] R.Q. Zou, H. Sakurai, S. Han, R.Q. Zhong, Q. Xu, *J. Am. Chem. Soc.* 129 (2007) 8402–8403.
- [5] Z. He, Z.M. Wang, S. Gao, C.H. Yan, *Inorg. Chem.* 45 (2006) 6694–6705.
- [6] X.M. Zhang, Z.M. Hao, W.X. Zhang, X.M. Chen, *Angew. Chem. Int. Ed.* 46 (2007) 3456–3459.
- [7] H. Li, M. Eddaoudi, M. O’Keeffe, O.M. Yaghi, *Nature* 402 (1999) 276–279.
- [8] H.K. Chae, D.Y. Siberio-Pérez, J. Kim, Y. Go, M. Eddaoudi, A.J. Matzger, M. O’Keeffe, O.M. Yaghi, *Nature* 427 (2004) 523–527.
- [9] R.V. Deun, P. Fias, P. Nockemann, K.V. Hecke, L.V. Meervelt, K. Binnemans, *Inorg. Chem.* 45 (2006) 10416–10418.
- [10] E.G. Moore, J. Xu, C.J. Jocher, E.J. Werner, K.N. Raymond, *J. Am. Chem. Soc.* 128 (2006) 10648–10649.
- [11] M.R. Shimpi, N. SeethaLekshmi, V.R. Pedireddi, *Cryst. Growth Des.* 7 (2007) 1958–1963.
- [12] Y.B. Dong, H.X. Xu, J.P. Ma, R.Q. Huang, *Inorg. Chem.* 45 (2006) 3325–3343.
- [13] L. Fan, E. Wang, Y. Li, H. An, D. Xiao, X. Wang, *J. Mol. Struct.* 841 (2007) 28–33.
- [14] W.G. Lu, J.Z. Gu, L. Jiang, C.Y. Jiang, C.Y. Su, T.B. Lu, *Chin. J. Inorg. Chem.* 22 (2006) 1977–1981.
- [15] Z.X. Lian, J. Cai, C.H. Chen, H.B. Luo, *Cryst. Eng. Commun.* 9 (2007) 319–327.
- [16] B. Liu, W. Chen, S. Jin, *Organometallics* 26 (2007) 3660–3667.
- [17] W. Starosta, H. Ptasiwicz-Bak, J. Leciejewicz, *J. Coord. Chem.* 56 (2003) 33–39.
- [18] M.A.S. Goher, R.J. Wang, T.C.W. Mak, *J. Cryst. Spectr. Res.* 20 (1990) 245–249.
- [19] S. Qin, S. Lu, Y. Ke, J. Li, X. Wu, W. Du, *Solid State Sci.* 6 (2004) 753–759.
- [20] J.H. Yang, S.L. Zheng, X.L. Yu, X.M. Chen, *Cryst. Growth Des.* 4 (2004) 831–836.
- [21] G.M. Sheldrick, SHELXL-97, Program for X-ray Crystal Structure Solution. University of Göttingen, Germany, 1997.
- [22] G.M. Sheldrick, SHELXL-97, Program for X-ray Crystal Structure Refinement, University of Göttingen, Germany, 1997.
- [23] P. Milart, K. Stadnicka, *Eur. J. Org. Chem.* (2001) 2337–2341.
- [24] D.K. Kumar, A. Das, P. Dastidar, *Inorg. Chem.* 46 (2007) 7351–7361.
- [25] V.T. Yilmaz, S. Hamamci, O. Buyukgungor, *Polyhedron* 27 (2008) 1761–1766.
- [26] Y. Chen, Z.G. Ren, H.X. Li, X.Y. Tang, W.H. Zhang, Y. Zhang, J.P. Lang, *J. Mol. Struct.* 875 (2008) 339–345.
- [27] V.J. Catalano, H.M. Kar, J. Garnas, *Angew. Chem. Int. Ed. Engl.* 38 (1999) 1979–1982.
- [28] A.M. Stadler, N. Kyritsakas, G. Vaughan, J.M. Lehn, *Chem. Eur. J.* 13 (2006) 59–68.
- [29] Y. Zhou, X. Zhang, W. Chen, H. Qiu, *J. Organomet. Chem.* 693 (2008) 205–215.
- [30] M.C. Munoz, A.B. Gaspar, A. Galet, J.A. Real, *Inorg. Chem.* 46 (2007) 8182–8192.
- [31] A. Bondi, *J. Phys. Chem.* 68 (1964) 441–451.
- [32] M. Jansen, *Angew. Chem. Int. Ed. Engl.* 26 (1987) 1098–1110.
- [33] C.-L. Chen, B.-S. Kang, C.-Y. Su, *Aust. J. Chem.* 59 (2006) 3–18.
- [34] A.L. Spek, PLATON, A Multipurpose Crystallographic Tool, Utrecht University, Utrecht, The Netherlands, 2001.
- [35] V. Swaminathan, L.C. Greene, *J. Lumin.* 14 (1976) 357–363.
- [36] F. Hung Low, K.K. Klausmeyer, *Inorg. Chim. Acta* 361 (2008) 1298–1310.
- [37] C.M. Che, M.C. Tse, M.C.W. Chan, K.K. Cheung, D.L. Phillips, K.H. Leung, *J. Am. Chem. Soc.* 122 (2000) 2464–2468.
- [38] K.J. Wei, J. Ni, J. Gao, Y. Liu, Q.L. Liu, *Eur. J. Inorg. Chem.* (2007) 3868–3880.
- [39] J. Tao, X. Yin, Z.B. Wei, R.B. Huang, L.S. Zheng, *Eur. J. Inorg. Chem.* (2004) 125–133.
- [40] C.C. Wang, C.H. Yang, S.M. Tseng, S.Y. Lin, T.Y. Wu, M.R. Fuh, G.H. Lee, K.T. Wong, R.T. Chen, Y.M. Cheng, P.T. Chou, *Inorg. Chem.* 43 (2004) 4781–4783.
- [41] A. Barbieri, G. Accorsi, N. Armaroli, *Chem. Commun.* (2008) 2185–2193.
- [42] H.H. Patterson, S.M. Kanan, M.A. Omary, *Coord. Chem. Rev.* 208 (2000) 227–241.
- [43] V.W.W. Yam, *Acc. Chem. Res.* 35 (2002) 555–563.
- [44] P. Cassoux, *Science* 291 (2001) 263–264.
- [45] S.L. Zheng, J.P. Zhang, X.M. Chen, Z.L. Huang, Z.Y. Lin, W.T. Wong, *Chem. Eur. J.* (2003) 3888–3896.
- [46] S.L. Zheng, J.P. Zhang, W.T. Wang, X.M. Chen, *J. Am. Chem. Soc.* 125 (2003) 6882–6883.